



**HAL**  
open science

# On geodesic paths and least-cost motions for human-like tasks

Adrien Datas, Pascale Chiron, Jean-Yves Fourquet

► **To cite this version:**

Adrien Datas, Pascale Chiron, Jean-Yves Fourquet. On geodesic paths and least-cost motions for human-like tasks. 2010 IEEE International Conference on Robotics and Biomimetics (ROBIO), Dec 2010, Tianjin, China. pp.1025-1031, 10.1109/ROBIO.2010.5723467 . hal-03956180

**HAL Id: hal-03956180**

**<https://hal.science/hal-03956180>**

Submitted on 24 Mar 2023

**HAL** is a multi-disciplinary open access archive for the deposit and dissemination of scientific research documents, whether they are published or not. The documents may come from teaching and research institutions in France or abroad, or from public or private research centers.

L'archive ouverte pluridisciplinaire **HAL**, est destinée au dépôt et à la diffusion de documents scientifiques de niveau recherche, publiés ou non, émanant des établissements d'enseignement et de recherche français ou étrangers, des laboratoires publics ou privés.



## Open Archive Toulouse Archive Ouverte (OATAO)

OATAO is an open access repository that collects the work of Toulouse researchers and makes it freely available over the web where possible.

This is an author-deposited version published in: <http://oatao.univ-toulouse.fr/>  
Eprints ID: 5369

**To link to this article:**

<http://dx.doi.org/10.1109/ROBIO.2010.5723467>

To cite this version : Datas, Adrien and Chiron, Pascale and Fourquet, Jean-Yves *On geodesic paths and least-cost motions for human-like tasks*. (2010) In : 2010 IEEE International Conference on Robotics and Biomimetics (ROBIO), 14-18 Dec 2010, Tianjin, China.

Any correspondence concerning this service should be sent to the repository administrator: [staff-oatao@inp-toulouse.fr](mailto:staff-oatao@inp-toulouse.fr)

# On geodesic paths and least-cost motions for human-like tasks

Adrien Datas, Pascale Chiron and Jean-Yves Fourquet

**Abstract**— We are interested in "human-like" automatic motion generation. The apparent redundancy of the humanoid wrt its explicit tasks lead to the problem of choosing a plausible movement in the framework of redundant kinematics. Some results have been obtained in the human motion literature for reach motion that involves the position of the hands. We discuss these results and a motion generation scheme associated. When orientation is also explicitly required, very few works are available and even the methods for analysis are not defined. We discuss the choice for metrics adapted to the orientation, and also the problems encountered in defining a proper metric in both position and orientation. Motion capture and simulations are provided in both cases. The main goals of this paper are : - to provide a survey on human motion features at task level for both position and orientation, - to propose a kinematic control scheme based on these features - to define properly the error between motion capture and automatic motion simulation.

## I. INTRODUCTION

Human motion generation is highly complex and is concerned with (at least):

- the way the tasks are imposed or characterized
- the way the numerous dof of the human kinematic chain are coordinated for a given task
- how internal dynamics are taken into account
- how interaction with the environment is modeled.

The work described here is devoted to the study of intrinsic properties of the task space and of the mapping at kinematic level between task and joint space. The motivation is not to neglect dynamics - essential in whole-body equilibrium for instance - but to describe a simple framework for plausible human-like motion generation, when dynamics are not decisive. The ideas are tested on sitting reach motions, for both translations and rotations task components.

Generally, the task is denoted by the evolution in space and time of the location  $X$  of dimension  $m$ . A reaching task consists in reaching a location  $X^f$  from  $X^0$ . The configuration  $q$  of the mechanical system is known when the value of all its  $n$  independent joints is known. If  $m < n$ , the motion problem is under-constrained, sometimes said "ill-posed" in human movement literature, and this setting is known as *kinematic redundancy*. Then, a multiplicity of joint velocities produce the same velocity in task space. The problem can be formulated as an optimization problem in configuration space and, inside this category of problems, minimum-norm solutions leads to weighted pseudo-inversion schemes [1].

A. Datas, P. Chiron and J-Y. Fourquet are with Laboratoire Génie de Production, LGP-ENIT, INPT, Un. de Toulouse, FRANCE  
{adrien.datas,  
pascale.chiron, jean-yves.fourquet}@enit.fr

Literature on the human movement analysis is mainly focused on reach motion and translation information. Very few works have studied the questions relative to the orientation of the hand or relative to the paths and motions in task space when reaching and grasping is concerned, or when translation and rotation of the end-effector are both imposed. Questions are numerous : they concern the geometry in task space (shape of paths, significant parameterisation [2] [3],...), and the temporal aspects (velocity profile, sequences of reach and grasp [4] [5] [6], simultaneous evolution of translation and rotation [7][8],...). Since coordination of translation and rotation is the focal point, time-scale and length-scale are obviously concerned. As a result of human motion studies, no "fundamental human motion principle" emerges but optimisation principles have proved to be useful guides.

In this paper, the focus is on seated reaching motions. The simulations are realized with a 23 Degrees Of Freedom (DOF) virtual human (Fig. 1). In the next section, translation paths are studied and a kinematics-based scheme is proposed when task path requires too much joint displacement. Section 3 presents a similar approach for rotations. Finally, the last section presents discuss the translation and rotation coordination. In every section, motion capture and simulation curves are provided.

## II. TRANSLATION CONSTRAINTS

### A. Distance, path and motion in task space

In this case,  $X$  is made of the cartesian coordinates  $X_p = (x, y, z)$  of a specific body (hand, head,...) and the natural way to measure length and distance is to use the Euclidean metric. Various authors have studied the reach motion in free space. In many cases reported in the litterature, the observed path is close to straight lines [9] [10] and the motion along the path exhibits a bell-shaped velocity profile [11] [12]. This behavior has been associated to integral criteria, first in task-space. Among them, the measures substantiate the *minimum hand jerk* solution [9] i.e. the solution  $X_p(t)$  that minimizes:

$$C = \frac{1}{2} \int_0^{t_f} \left\{ \left( \frac{d^3x}{dt^3} \right)^2 + \left( \frac{d^3y}{dt^3} \right)^2 + \left( \frac{d^3z}{dt^3} \right)^2 \right\} dt \quad (1)$$

where  $t_f$  is the total duration of the motion and under the constraints that the derivatives  $\frac{d^2x}{dt^2}, \frac{d^2y}{dt^2}, \frac{d^2z}{dt^2}, \frac{dx}{dt}, \frac{dy}{dt}, \frac{dz}{dt}$  all equal zero at both endpoints.

In fact, the Calculus of Variations [13] enables us to conclude that since there is no coupling between the Cartesian coordinates, the path solution of (1) is naturally a straight

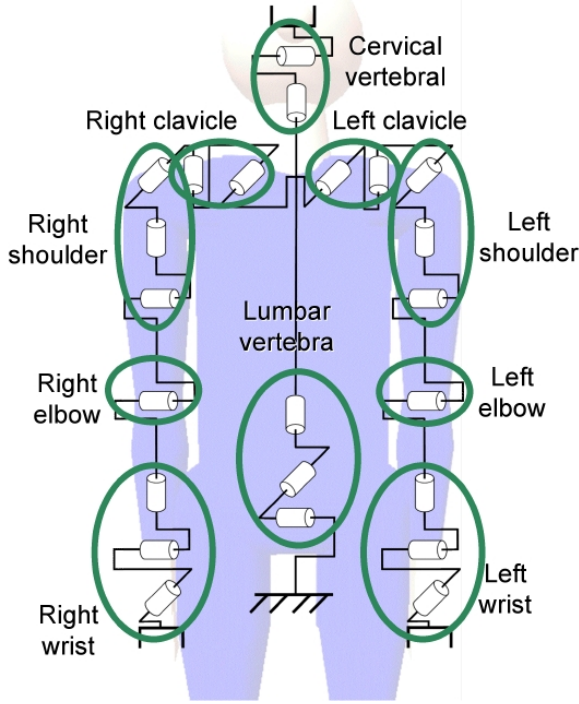


Fig. 1. virtual human kinematic structure

line. If this path  $X_p(s)$  is parameterized by its curvilinear abscissa  $s$  ( $s \in [0, 1]$ , and  $X_p(s = 0) = X_p^0$  and  $X_p(s = 1) = X_p^f$ ), then the minimum hand jerk impose the following time law along the path:

$$s(t) = a_5 t^5 + a_4 t^4 + a_3 t^3 + a_0, 0 \leq t \leq t^f \quad (2)$$

where the coefficients  $a_i$  depend on the endpoints value  $X_p^0$  and  $X_p^f$  and on  $t^f$ .

This solution provides the minimum distance path - the geodesic - in the usual Cartesian metrics covered with a smooth time profile verifying the minimum jerk solution along this straight line.

Thus a way to program human-like simulation for a variety of position tasks is to impose a straight line  $X_p(s)$  and the  $s(t)$  law defined in relation (2) on this straight line.

In fact, several authors have shown that the reference path is not always a straight path and some of them attempted to define new criteria in order to explain these discrepancies. On the one hand, one may think that evolution has led to render the human locomotor apparatus really efficient and turn him able to follow the most efficient paths in Cartesian space : the straight line. Remark that statistical methods popularized in industrial cycle-time measurement such as MTM implicitly include this fact since the cycle-time in usual workplaces is only related to distance of reach [14] [15] [16] [17]. On the other hand, we know that kinematic chains are not isotropic motion generators in Cartesian space. Thus, intuitively, one can infer that there is a preferred workspace zone in which the path is a straight line, and other zones in which the

mechanical constraints induced by the nature of kinematic chains will render really difficult to follow a straight line. Here, the matter is not so much to ask if the optimization criterion acts in Cartesian space or in Joint Space [18] [19] but rather how to reproduce a trade-off between the task efficiency and the constraints induced by the mechanical structure.

### B. Space mappings and mixed criteria

The relation between the respective first order variations  $\delta X_p$  and  $\delta q$ , or the exact relation between the velocities  $\dot{X}_p$  and  $\dot{q}$ , writes as a linear map:

$$\delta X_p = J_p \delta q \quad \text{or} \quad \dot{X}_p = J_p \dot{q} \quad (3)$$

where  $J_p = J_p(q)$  is the  $3 \times n$  Jacobian matrix associated to the task  $X_p$ . This mapping is configuration-dependent and does not provide an isotropic transformation from joint space to task space. The properties of this mapping are enlightened by its singular value decomposition (SVD) [20]. SVD provides the means to analyse the amount of joint displacement necessary to move in a given direction in task space. SVD of  $J_p$  writes:

$$J_p = U \Sigma V^T \quad (4)$$

where:  $U = [u_1 \ u_2 \dots u_m]$  is an orthonormal basis of for the tangent vectors to the task space,  $V = [v_1 \ v_2 \dots v_n]$  is an orthonormal basis of the tangent space to the configuration space,  $\Sigma = \text{diag}\{\sigma_1, \sigma_2, \dots, \sigma_p\}$  is a  $(m \times n)$  diagonal matrix with rank  $p = \min\{m, n\}$  and the singular values  $\sigma_i$  of  $J_p$  are arranged such that  $\sigma_1 \geq \sigma_2 \geq \dots \geq \sigma_p \geq 0$ .

The geometrical meaning of this decomposition is :  $J_p$  maps a unit ball in the tangent space to the task space into a  $p$ -dimensional ellipsoid in the tangent space to the configuration space. This ellipsoid has principal axes  $u_i$  with length  $\sigma_i$ . Remark that the  $\{u_i ; i = 1, \dots, p \leq m\}$  form a basis for the range of  $J_p$  and the  $\{v_i ; i = p + 1, \dots, n\}$  form a basis of the kernel of  $J_p$ .

Thus, a significant difference of value among the  $\sigma_i$  implies that the amount of joint displacement consumed for a given norm of task displacement in task space varies with the direction and that some directions in task space are really easier to follow.

Thus, on the one hand, one may think that human motion will occur in straight line if the task path does not require a large amount of joint motion. On the other hand, some configurations are such that task displacement in a certain direction requires a really high amount of joint motion : in this latter case, at least one singular value takes a significant smaller value and straight paths are not necessarily efficient.

### C. The motion scheme

The proposed approach consists in choosing straight lines as initial guesses for the Cartesian path and to adapt this guess depending on the SVD. Thus, the simulated movements are built upon optimisation in path space under the condition of a reasonable expense in joint space.

This program is realised on the basis of a kinematic control scheme where lower singular-values filtering acts when SVD detects that the straight line is too costly at joint level.

The control scheme is the following :

$$\delta q = J_{W,F}^+ \delta X_p + P_p z \quad (5)$$

where the main task consists in following the Cartesian path and  $P_p z$  is a secondary task built upon :

- the projector  $P_p$  into the null space of  $J$ ,
- an  $n$ -dimensional vector  $z$  computed as the scaled gradient of a potential field that enables to take into account inequality constraints such as joint limit avoidance and reference posture adjustment.

The main task uses the weighted and filtered pseudoinverse of  $J_p$  [1] :

$$J_{W,F}^+ = W^{-1} J^t (JW^{-1} J^t + F)^{-1} \quad (6)$$

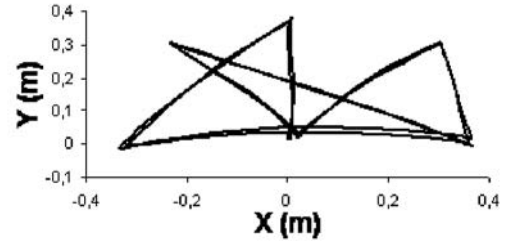
where  $W$  is the inertia matrix and  $F$  stands for the  $m \times m$  filtering matrix [21] computed by :

$$F = \sum_{i=1}^m (\alpha_i^2 u_i u_i^t) \quad (7)$$

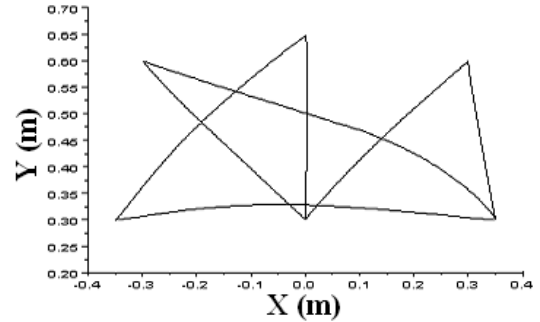
In this matrix, the respective weight  $\alpha_i$  of the  $u_i$  components is directly related to the value of  $\sigma_i$ . A threshold on  $\sigma_i$  value has been computed from captured motions paths [22], by computing singular values for straight and curved Cartesian paths. If the singular value  $\sigma_i$  is upper this threshold, then  $\alpha_i = 0$ , else  $\alpha_i$  takes a non-zero value along a continuous  $\alpha_i(\sigma_i)$  profile.

#### D. Motion capture and simulation results

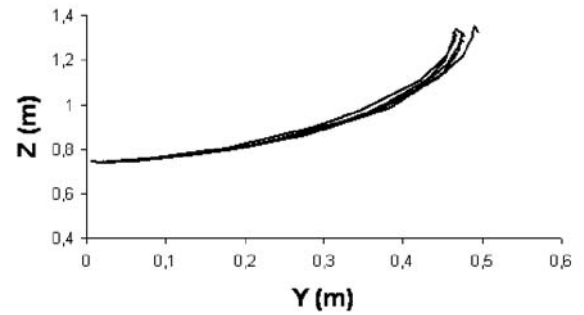
Motion captures have been performed on two test cases (see Fig. 2): first, a literature [9] [11] sequence of reaching motions in the horizontal plane and, second, a movement on the vertical plane where the initial posture is such that the arm is stretched along the body and subjects have to reach a target in front of them. The first example is representative of measured paths in many experiments of the literature : paths are approximate straight lines and the hand velocity matches the bell-shaped profile of minimum hand jerk criterion. The second example shows that kinematics changes the hand path depending on the configuration. In simulation, the same tuning of our control scheme exhibits similar path features (see Fig. 2) : it produces straight lines motions when it is efficient to follow them and it switches to curved paths when kinematics prescribe a locally better path. Comparizon of solutions, captured and simulated, are made through the usual Cartesian distance measure through the Linearity index (LI) [7]. The linearity index is a measure of path curvature. The smaller the LI, the straighter the path. The values obtained for this index are significant in both examples (for instance, test 2 : mean captured LI = 18,13 % with variation in the interval [13.65, 22.47] ; simulated LI = 19,45%).



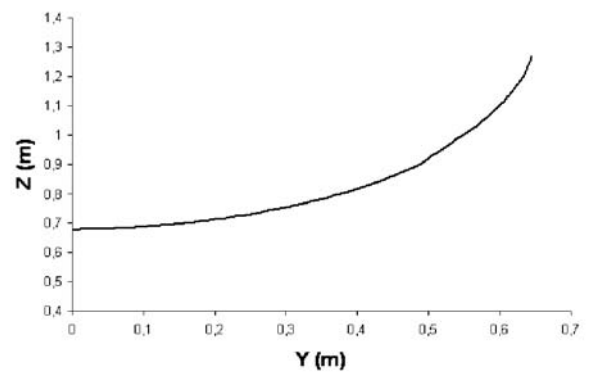
Test 1 : path of the hand for captured motion



Test 1 : path of the hand for simulated motion



Test 2 : path of the hand for captured motion



Test 2 : path of the hand for simulated motion

Fig. 2. Hand translation paths

### III. ROTATION CONSTRAINTS

Human manipulation tasks (touch, grasp, carry) is such that the position and orientation of the hand(s) is partially or totally known. If the task presents a symmetry, one rotation can be left free, but in many cases it is desirable to impose the orientation of the hands as the result of the definition of a task.

#### A. Distance, path and motion in task space

Intrinsically, rotations are elements of  $SO(3)$  (the Special Orthogonal Group of dimension 3), a 3-dimensional differential manifold with a Lie group structure. A point in this manifold is computed in coordinates by several choices, through various parameterizations. Among them, some are made of surabondant not independent components (rotation matrices), some other are endowed with a minimal number of components (3-angles systems : Euler, Bryant, Yaw-Pitch-Roll,...) but also with singularities ("gimbal lock"). Axis-Angle representation, unit quaternions, exponential map are formalisms that are really close to the canonical coordinates of  $SO(3)$ . Here, the following developments mainly use the exponential map formalism [23] [24].

We try to follow the same vein as for the translations. Then, it is necessary to first define a least distance path - a geodesic - on  $SO(3)$ , and second to interpolate a minimum jerk time-evolution along this path.

Let denote  $R = (r_{ij})$  a rotation matrix. Since Euler [24], we know that it is possible to transform a rotation matrix (or an orthonormal vector frame)  $R_0$  into a rotation (or another vector frame)  $R_1$  by defining a vector  $w$  around which an amount of rotation  $\Theta \in [0, 2\pi)$  is performed. The exponential map formalism exploits this axis-angle representation.

Let us denote  $[\hat{a}]$  the skew-symmetric  $3 \times 3$  matrix derived from the  $\mathbb{R}^3$  vector  $a$  that enables to transform the cross-product in a matrix multiplication  $\mathbf{a} \times \mathbf{b} = [\hat{a}]\mathbf{b}$ . Then  $\dot{R} = w \times R$  writes  $\dot{R} = [\hat{w}]R$ . The solution of this linear matrix differential equation is  $R(t) = \text{expm}([\hat{w}]t)R(0)$  where  $\text{expm}$  stands for matrix exponential and is given for  $\|w\| = 1$  by:

$$\text{expm}([\hat{w}]\theta) = I + [\hat{w}]\sin\theta + [\hat{w}]^2(1 - \cos\theta) \quad (8)$$

In the same way, it is possible to prove the existence of  $(w, \Theta)$  with  $\|w\| = 1$  and  $\Theta \in [0, 2\pi)$  such that the motion between two orientations  $R_0$  and  $R_1$  is given by :  $R_1 = \text{expm}([\hat{w}]\Theta)R_0$ . The geodesic on  $SO(3)$  between  $R_0$  and  $R_1$  is obtained by rotating around  $w$  with a  $\Theta$  amount and the equation (8) provides a natural way to interpolate on the geodesic.

Conversely, one can write  $w\theta = \text{logm}(R(t)R_0^t)$  where  $\text{logm}$  stands for the matrix logarithm and is given by :  $\text{logm}(R) = \frac{\Theta}{2\sin\Theta}(R - R^t)$  with  $\Theta = \cos^{-1}\left(\frac{\text{trace}(R)-1}{2}\right)$

Note that  $w$  can be obtained in various ways (from the rotation matrices or quaternions, for instance) and is given by the formula (with  $R = R_1R_0^t$ ) :

$$w = \text{logm}(R) = \frac{1}{2\sin\Theta} \begin{bmatrix} r_{32} - r_{23} \\ r_{13} - r_{31} \\ r_{21} - r_{12} \end{bmatrix}$$

The distance between two rotations is the length of the shortest path between them. It is then computed along geodesics. In  $SO(3)$ , this distance  $d_r$  between two rotations  $R_0$  and  $R_1$  is given by :

$$d_r(R_0, R_1) = \|\text{logm}(R_0^t R_1)\|_{fro}$$

where  $\|A\|_{fro} = \text{trace}(\sqrt{A^t A}) = \sqrt{(\sum_i \sigma_i^2)}$  is the Frobenius norm of the matrix  $A$ .

Then, if  $\theta$  varies linearly as a function of the time ( $\theta(t) = \mu t + \nu$ ), the motion is a linear interpolation from  $R_0$  to  $R_1$  along the geodesic. This simple solution is the one provided by the *slerp* algorithm [25] popularized with unit quaternions. It provides a constant velocity evolution on the geodesic. From the physics, such a behavior seems unnatural since it requires infinite acceleration at the beginning and at the end. Remark that translation and rotations results from the same biomechanic system, it is plausible that the time evolution of the variables obeys the same smoothness properties. Then, again minimizing the jerk along the geodesic is the choosen solution and thus :

$$\theta(t) = a_5 t^5 + a_4 t^4 + a_3 t^3 + a_0, 0 \leq t \leq t^f$$

#### B. space mapping and optimisation

Tangent vectors to  $SO(3)$  are related to joint velocities by the canonical linear map :

$$w = J_r \dot{q} \quad (9)$$

where  $J_r$  is a  $3 \times n$  matrix.

Then, the animation problem requires first that  $w$  and  $\theta(t)$  be given and second to provide a generalized inversion scheme for the linear system (9). Again, the norm of the tangent vectors in both spaces can be efficiently computed by SVD which gives a local measure of preferred directions in task space for a given configuration.

#### C. Motion capture results

The idea is to experiment a simple rotation without translation of the reference point. We ask the subjects to rotate the pose of the hand between two drawn orientations superposed at the same position. The motion capture results are presented in the figures 3 and 4.

The figure 3 shows that the time profile for a simple movement of rotation around the vertical axis is really similar to the minimum jerk profile. The figure 4 represents the time evolution of the rotation (from left to right) at regularly spaced instants and we remark that the captured motion is slightly different from the geodesic. The measured maximum distance is :  $d_{r_{max}} = 0.152$ . Finally, remark that it is quite difficult and unusual to perform a pure rotation movement.

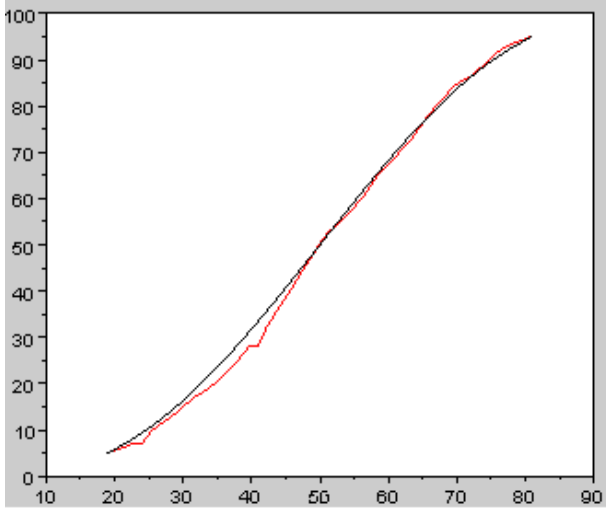


Fig. 3. Experiment 2 : Comparison between time evolution of captured rotation of the hand (red) and the unidimensional minimum jerk curve (black).

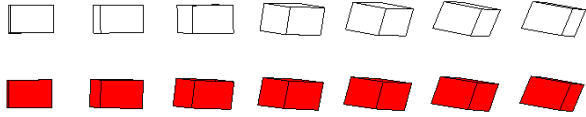


Fig. 4. Experiment 2 : Boxes representative of the time evolution of the rotation. White boxes (top) represent the captured movement. Orange boxes (down) represent the rotation geodesic.

#### IV. COMBINING ROTATIONS AND TRANSLATIONS

##### A. Discussion

The task simulation amounts to the definition of the interpolation laws for both the position of a particular point of the hand (the Tool Center Point (TCP)) and the orientation of a body-fixed frame. Such a composite object lives in  $SE(3)$ , the Special Euclidean group of dimension 3. The associated differential kinematics writes :

$$\begin{bmatrix} v \\ \omega \end{bmatrix} = \begin{bmatrix} J_p \\ J_r \end{bmatrix} \dot{q} \quad (10)$$

Different possibilities arise in choosing the solution of this linear system. On one side, one may think that translation and rotation follow their own rule, independently in two parallel spaces,  $\mathbb{R}^3$  for the Cartesian coordinates,  $SO(3)$  for the orientation parameters. Intrinsic metric and closed-form geodesics are available in each space. Following this idea leads to obtain a straight line motion in Cartesian space for the TCP and a geodesic in  $SO(3)$  for the frame attached to the body. We may think that this independence is dubious. In fact, beyond the fact that this problem is solvable in a well-posed setting with natural metrics, at least two other arguments speak for this solution. Firstly, this decoupling is observed naturally in the motion of bodies : in absence of external forces, the linear and angular velocities keep constant values and the resulting path follow in parallel the geodesics of  $\mathbb{R}^3$  and  $SO(3)$ . Second,  $SE(3)$  is not the

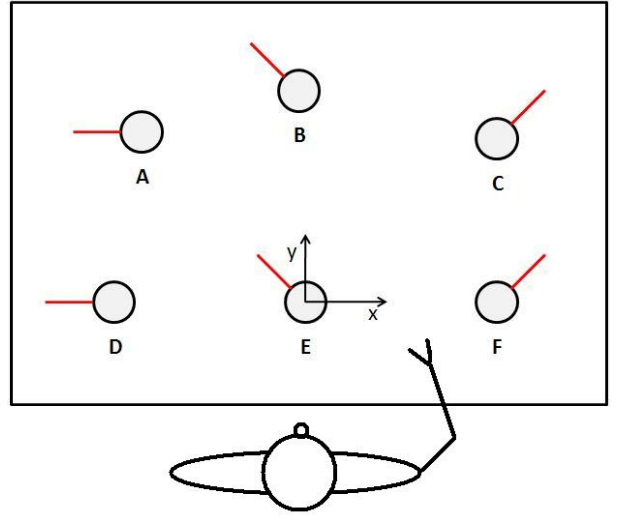


Fig. 5. Experiment 3 : position and rotation constraints

cross-product of  $\mathbb{R}^3$  and  $SO(3)$  and there is no natural (i.e. no bi-invariant) metric on it [26]. Thus, choosing a metric in  $SE(3)$  requires to weight two mathematical objects of different nature with an unique measure of length. Such a weighting has no intrinsic meaning from the geometric point of view. It amounts to choose a Riemannian metric [27] on  $SE(3)$  defined by a block-diagonal matrix  $W$  related to the length  $l$  by:

$$W = \begin{bmatrix} \beta I & 0 \\ 0 & \delta I \end{bmatrix} \quad \text{and} \quad l = \sqrt{\sum \beta_{ij} v_i v_j + \sum \delta_{ij} w_i w_j} \quad (11)$$

This is equivalent to the choice of a length scale between  $s$  and  $\theta$ . This choice may be motivated by different reasons and the synchronization of translations and rotations may be viewed as time or/and length scale.

In some captured motions, we observe paths that are fairly far from the geodesics, for the translation or the rotation part, or for both. This is in particular the case for motion in which the amount of rotation is really important, and should require that the translation does not occur along a straight line. Thus, again the geometry of the task space is not the sole decisive factor in the generation of human motion. The way rotation and translation constraints interfere in determining a good path in  $SE(3)$  is not easy to understand. If one applies the filtering scheme illustrated for the translation parameters, it must be kept in mind that the singular values of the global map (10) are dependent on the choice of length made in (11).

##### B. Motion capture and simulation

The experiment of paragraph II is modified in the way depicted at figure 5 and tested with 8 subjects. Each subject has to follow the sequence given by (12).

$$E \Rightarrow B \Rightarrow D \Rightarrow F \Rightarrow C \Rightarrow E \Rightarrow A \Rightarrow F \quad (12)$$

For illustrating purposes, we focus here on two movements depicted in red in the figures : a first one for which the

Point	position X	position Y	orientation
A	-25	30	+90
B	0	25	+45
C	30	29	-45
D	-30	0	+90
E	0	0	+45
F	30	0	-45

TABLE I  
HAND POSITIONS AND ROTATIONS

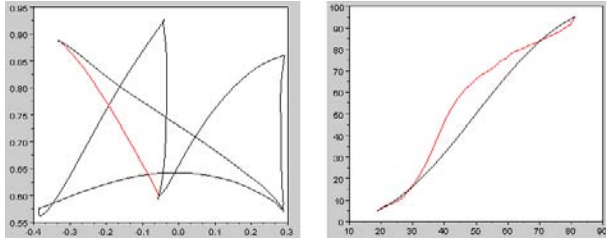


Fig. 6. Experiment 3.1 : (a) - translation part of the global sequence of movements (black) and of the studied movement (red) (b) - Comparison between the time evolution of the hand orientation (red) and the minimum jerk (black).

translation observed is close to a straight line, and a second one for which this translation occurs along a curve really different from a straight line. In both movements, the time and space evolution are studied.

The first movement is represented in figures 6 and 7.

Contrary to the observations for the pure rotation movement, the figure 6 shows that the time profile may be different than the minimum jerk profile. Moreover, the figure 7 shows that the human movement does not always follow the shortest rotation path. The distance between the shortest path and this movement are  $LI = 4,16\%$  for the position and  $d_{r_{max}} = 0,45$  for the rotation.

The second captured movement is represented in the figures 8 and 9.

Here, the rotation time profile is identical to a minimum jerk profile (see figure 8) but the rotation does not follow the rotation shortest path (see figure 9). The differences between the shortest path and the captured movement are  $LI = 10,16\%$  for the position and  $d_{r_{max}} = 0,35$  for the rotation.

Both movements are simulated with the kinematic control scheme described in the section II. The reference path are the geodesics in rotation and translation, and these path are covered with a minimum jerk profile after un length-scale

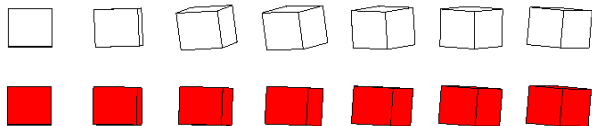


Fig. 7. Experiment 3.1 : Boxes representative of the time evolution of the rotation. White boxes (top) represent the **captured** movement. Orange boxes (down) represent the rotation geodesic.

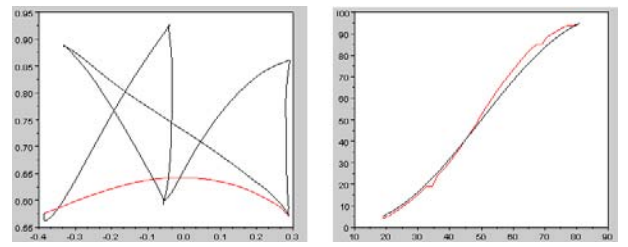


Fig. 8. Experiment 3.2 : (a) - translation part of the global sequence of movements (black) and of the studied movement (red) (b) - Comparison between the time evolution of the hand orientation (red) and the minimum jerk (black).

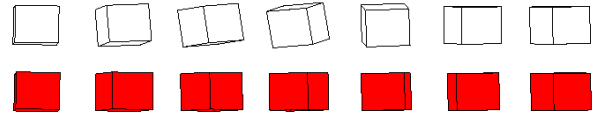


Fig. 9. Experiment 3.2 : Boxes representative of the time evolution of the rotation. White boxes (top) represent the **captured** movement. Orange boxes (down) represent the rotation geodesic.

in order to synchronize rotation and translation components. SVD filtering is applied in order to take into account the cost in joint space. The results of the first movement are given in the figures 10 and 11 ; the results of the second one are given in the figures 12 and 13.

The simulation of the experiment 3.1 has a straight deformation about 1,97%. The measured maximum distance for the rotation is :  $d_{r_{max}} = 0,027$ . For the experiment 3.2, the results are  $LI = 5,32\%$  for the position and a distance of  $d_{r_{max}} = 0,03$  for the rotation. These simulations are dependent on the tuning of the SVD filtering that amounts to weight rotation and translation on one side, internal kinematic constraints on the other. It is shown that various features can be conserved (SVD deformation in translation,

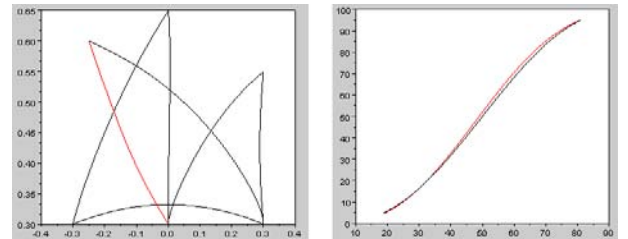


Fig. 10. Experiment 3.1 (**simulation**) : (a) - translation part of the global sequence of movements (black) and of the studied movement (red) (b) - Comparison between the time evolution of the hand orientation (red) and the minimum jerk (black).

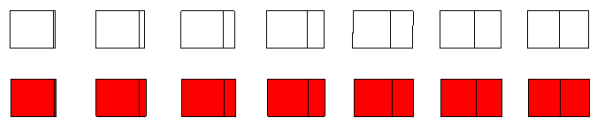


Fig. 11. Experiment 3.1 : Boxes representative of the time evolution of the rotation. White boxes (top) represent the **simulated** movement. Orange boxes (down) represent the rotation geodesic.

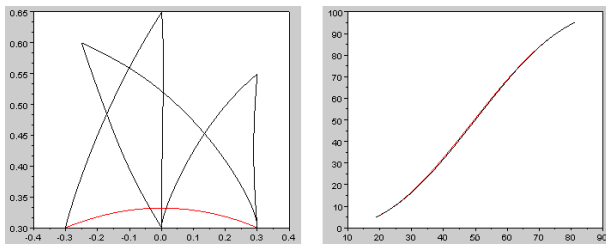


Fig. 12. Experiment 3.2 (simulation) : (a) - translation part of the global sequence of movements (black) and of the studied movement (red) (b) - Comparison between the time evolution of the hand orientation (red) and the minimum jerk (black).

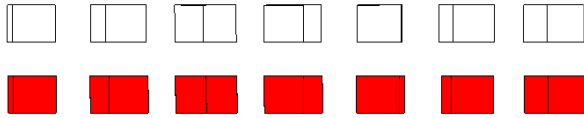


Fig. 13. Experiment 3.2 : Boxes representative of the time evolution of the rotation. White boxes (top) represent the **simulated** movement. Orange boxes (down) represent the rotation geodesic.

minimum jerk rotation time profile) but that it is difficult to predict which component is prevalent in a given movement. Much work remains necessary to analyze which metrics are pertinent and how space and time constraints interact.

## V. CONCLUDING REMARKS

This work aims at showing how complex is the global study of human motion both in time and space dimensions. Metrics and shortest paths have been defined and tested in real and simulation. Many cases arise and some of the key features that appear in the real movements can be reproduced or predicted by a kinematic control scheme. Nonetheless, shortest paths in the separate metrics, for rotation and translation, are not always observed. Minimum jerk time profile is sometimes slower than the observed time profile, and much work remains necessary to analyze how space and time constraints interact. This may prove the need for the definition of coupled metrics in  $SE(3)$  or for a proper weighting between geometric cost in task space, geometric cost in joint space and internal dynamics constraints.

## REFERENCES

- [1] A. Ben-Israel and T.N.E Greville. *Generalized inverse theory*. Springer, 2003.
- [2] S.B. Choe and J.J. Faraway. Modeling head and hand orientation during motion using quaternions. *Proceeding of the SAE Digital Human Modeling for Design and Engineering Conference*, June 15-17 2004.
- [3] M.R. Pierrynowski and K.A. Ball. Oppugning the assumptions of spatial averaging of segment and joint orientations. *Journal of Biomechanics*, 42:375–378, 2009.
- [4] F. Lacquaniti and J.F. Soechting. Coordination of arm and wrist motion during a reaching task. *The Journal of Neuroscience*, 2(4):399–408, 1982.
- [5] J. Fan, J. He, and S.I. Helms Tillery. Control orientation and arm movement during reach and grasp. *Experimental Brain Research*, 171(3):283–296, 2006.
- [6] C. Hesse and H. Deubel. Changes in grasping kinematics due to different start postures of the hand. *Human Movement Science*, 28(4):415 – 436, 2009.

- [7] X. Wang. Three-dimensional kinematic analysis of influence of hand orientation and joint limits on the control of arm postures and movements. *Biological Cybernetics*, 80:449–463, 1999.
- [8] N. Bennis and A.R. Brami. Coupling between reaching movement direction and hand orientation for grasping. *Brain Research*, 952(2):257 – 267, 2002.
- [9] T. Flash and N. Hogan. The coordination of arm movements: An experimentally confirmed mathematical model. *Journal of Neuroscience*, 5(7):1688–1703, 1985.
- [10] J.F. Soechting and F. Lacquaniti. Invariant characteristics of a pointing movement in man. *The Journal of Neuroscience*, 1(7):710–720, 1981.
- [11] P. Morasso. Spatial control of arm movements. *Experimental Brain Research*, 42:223–227, 1981.
- [12] C.G. Atkeson and J.M. Hollerbach. Kinematic features of unrestrained arm movements. *Journal of Neuroscience*, 5:2318–2330, 1985.
- [13] I.M. Gelfand and S.V. Fomin. *Calculus of variations*. Dover, 2000.
- [14] G. J. Stegemerten H. B. Maynard and J. L. Schwab. *Methods-time measurement*. McGraw-Hill industrial organization and management series, N. Y., 1948.
- [15] F.M. Kuhn and W. Laurig. Computer-aided workload analysis using MTM. In *Computer-aided ergonomics - A researcher s guide*. Taylor and Francis, 1990.
- [16] J. Laring, M. Forsman, R. Kadefors, and R. Ortengren. Mtm-based ergonomic workload analysis. *International Journal of Industrial Ergonomics*, 30(3):135 – 148, 2002.
- [17] L. Ma, W. Zhang, H. Fu, Y. Guo, D. Chablat, and F. Bennis. A framework for interactive work design based on digital work analysis and simulation. *Human Factors and Ergonomics in Manufacturing and Service Industries*, abs/1006.5226, 2010.
- [18] S.A. Engelbrecht. Minimum principles in motor control. *Journal of Mathematical Psychology*, 45:497–542, 2001.
- [19] M. Svinin, Y. Masui, Z-W. Luo, and S. Hosoe. On the dynamic version of the minimum hand jerk criterion. *J. Robot. Syst.*, 22:661–676, 2005.
- [20] G.H. Golub and C.F. Van Loan. *Matrix computations*. John Hopkins studies in Mathematical Sciences, 1983.
- [21] A.A. Maciejewski. Motion simulation: Dealing with the ill-conditioned equations of motion for articulated figures. *IEEE Comput. Graph. Appl.*, 10(3):63–71, 1990.
- [22] V. Hue, J.Y. Fourquet, and P. Chiron. On realistic human motion simulation for virtual manipulation tasks. In *10th International Conference on Control, Automation, Robotics and Vision*, pages 167 –172, dec. 2008.
- [23] F.C. Park and B. Ravani. Smooth invariant interpolation of rotations. *ACM Trans. Graph.*, 16(3):277–295, 1997.
- [24] R.M. Murray, S. Sastry, and L. Zexiang. *A Mathematical Introduction to Robotic Manipulation*. CRC Press, Inc., Boca Raton, FL, USA, 1994.
- [25] K. Shoemake. Animating rotation with quaternion curves. *SIGGRAPH Comput. Graph.*, 19(3):245–254, 1985.
- [26] M. Zefran and V. Kumar. Planning of smooth motions on  $se(3)$ . In *Proceedings of the 1996 IEEE International Conference on Robotics and Automation*, Minneapolis, Minnesota, April 1996.
- [27] S. Arimoto, M. Yoshida, M. Sekimoto, and K. Tahara. A riemannian geometry approach for control of robotic systems under constraints. *SICE Journal of Control, Measurement, and System Integration*, 2(2):107–116, 2009.